UC Berkeley
UC Berkeley Previously Published Works

Title
Self-Combustion Synthesis of Novel Metastable Ternary Molybdenum Nitrides

Permalink
https://escholarship.org/uc/item/8bc4t20d

Journal
ACS Materials Letters, 1(1)

ISSN
2639-4979

Authors
Odahara, Jin
Sun, Wenhao
Miura, Akira
et al.

Publication Date
2019-07-01

DOI
10.1021/acsmaterialslett.9b00057

Peer reviewed

Self-combustion synthesis of novel metastable ternary molybdenum nitrides

Jin Odahara,[a] Wenhao Sun,[b*] Akira Miura,[c*] Nataly Carolina Rosero-Navarro,[c] Masanori Nagao,[d] Isao Tanaka,[d] Gerbrand Ceder,[b,e] Kiyoharu Tadanaga[c]

[a] Graduate School of Chemical Sciences and Engineering, Hokkaido University, Sapporo 060-8628, Japan.

[b] Materials Sciences Division, Lawrence Berkeley National Laboratory, Berkeley, CA 94720, US

[c] Faculty of Engineering, Hokkaido University, Sapporo 060-8628, Japan.

[d] Center for Crystal Science and Technology, University of Yamanashi, Kofu 400-8511, Japan.

[e] Department of Materials Science and Engineering, UC Berkeley, Berkeley, California 94720, USA

Supporting Information Placeholder

ABSTRACT: Ternary metal nitrides are a promising class of functional materials, but their variety has been limited by the challenging nature of nitride synthesis. Here, we demonstrate a facile self-combustion synthesis route to novel ternary molybdenum nitrides. The room temperature mixing of $NaNH_2$, $MoCl_4$, and $3d$ transition metal chlorides—such as $MnCl_2$, $FeCl_3$, and $CoCl_2$—initiates a highly exothermic metathesis reaction, which is thermodynamically driven by the formation of stable $NaCl$, N_2, and NH_3 byproducts. The rapid combustion reaction yields ternary rocksalt γ-$TM_xMo_{1-x}N_{0.5}$ nanoparticles (TM=Mn, Fe, Co) in just a few seconds. We calculate from DFT that these disordered ternary molybdenum nitrides are thermodynamically stable under the high-temperatures which they form, but are remnantly metastable when quenched to ambient conditions. Introducing Mn, Fe, and Co into γ-Mo_2N is found to change its magnetic properties and to enhance its oxygen reduction catalytic activities. Our work demonstrates self-combustion synthesis as a simple but powerful route for the realization of novel ternary intermetallic nitrides with emergent functionality.

Introduction

Ternary metal nitrides are an exciting class of functional materials,[1-4] and have found applications as super hard materials,[5-6] magnetic media,[7-9] catalysts,[10-11] semiconductors,[12-13] and more. Mixed-transition metal (TM) nitrides have been reported, such as Fe_xWN_2,[14-15] $MnMoN_2$,[14] and others,[14, 16] but they are relatively rare compared to ternary alkali-TM-nitrides.[1,4, 17-19] Nevertheless, these early-TM nitrides, such as molybdenum nitrides, exhibit high chemical stability, which can be attributed to strong metal-nitrogen and metal-metal bonding.[20] Of the known mixed-TM nitrides, many have been synthesized by ammonolysis of oxide precursors, however, this process often requires long-term heat treatment at a narrow temperature range and a large amount of toxic ammonia gas.[14] Various other approaches have been developed for the synthesis of ternary nitrides, for example, thermal decomposition of a metal-hexamethylenetet-ramine complex,[21] mechanochemical alloying,[22] or solid-state reactions using NaN_3.[23] Despite these great efforts to synthesis new nitride materials, materials exploration in this space remains a challenging issue. To facilitate the discovery of new nitride materials, novel synthetic approaches are desired.

Self-combustion synthesis involves combining an alkali or alkaline earth metal compound and a metal halide, which drives a highly exothermic reaction that results in nanomaterials, such as nanocrystals and porous materials.[24-25] These double ion-exchange metathesis reactions are thermodynamically driven by the formation of stable byproducts,[26-32] which can facilitate the synthesis of compounds with otherwise small formation energies. To illustrate this point, Table 1 compares the reaction thermodynamics between the ammonolysis of MoO_3 to Mo_2N,[33] versus the self-combustion synthesis of Mo_2N from $NaNH_2$ and $MoCl_4$ precursors. The oxide ammonolysis reaction is enthalpically un-favorable, but can be entropically-driven at high temperatures by the production of 3.5 moles of gas. On the other hand, the self-combustion metathesis reaction is highly exothermic and proceeds spontaneously even at room temperature. The resulting alkali halide salt byproducts can be removed by simply washing the reaction products with water or an-other polar solvent.

These self-combustion synthesis routes have been reported for several nitride compounds; for example, the reaction between $ZrCl_4$ and Li_3N produces ZrN with the formation of stable $LiCl$ as a byproduct,[34] and we recently re-ported the self-combustion synthesis of barium niobium perovskite oxynitride from $Ba(OH)_2$, $NbCl_5$, and $NaNH_2$.[35] For the most part, metathesis reactions in the nitrides space have primarily focused on binary nitrides, or alkali ternary nitrides such as Li_2SiN_2.[36] Ternary mixed-transition metal ternary nitrides have not been explored as readily, despite their importance as superhard materials, superconductors, and catalysts. In this work, we report on the self-combustion

synthesis of new ternary mixed-metal molybdenum nitrides in the rocksalt structure. We focus on molybdenum nitrides because molybdenum is the most effective transition metal for forming ternary metal nitrides[1], and because of the excellent performance of molybdenum nitrides in catalytic applications.[37-39] The reaction between molybdenum chloride, $3d$ transition metal chlorides and sodium amide proceeded instantly, producing novel ternary molybdenum nitrides in just a few seconds. The temperature profiles of these combustion reactions exhibit rapid heating and quenching, which we demonstrate is able to produce metastable ternary $TM_xMo_{1-x}N_{0.5}$ compounds isostructural to the high-temperature γ-Mo_2N polymorph. Nitrides are the most metastable class of inorganic materials,[40] and our work here provides a simple but powerful route to this compelling class of functional materials.

Experimental and computational

Self-combustion synthesis of ternary molybdenum nitrides initiated from a reaction between $MoCl_4$, $NaNH_2$, and 3d transition metal chlorides. Preliminary experiments in optimizing Mo-Cl precursors found that the reaction of $MoCl_5$ (Wako, 99.5%) with $NaNH_2$ at room temperature formed γ-Mo_2N and δ–MoN (Figure S1). On the other hand, a reaction with $MoCl_3$ precursors (Aldrich, 99.95%) did not initiate at room temperature. However, $MoCl_4$ was found to be an effective starting precursor for the combustion synthesis of single-phase ternary molybdenum nitrides. Note that $MoCl_4$, $MoCl_5$ and $NaNH_2$ powders are moisture-sensitive and should be handled in a glove box with inert atmosphere.

Firstly, $MoCl_5$ and $MoCl_3$ were mixed in Ar-filled glove box. Then the mixture was heated at 543 K for 12 h in a vacuum sealed glass tube and subsequent heating at 433 K for 30 min under vacuum to obtain $MoCl_4$. The Teflon-lined autoclave with an inner volume of 70 ml (Yanako, AD-70) was heated at 493 K overnight to remove any water before the synthesis reaction of molybdenum nitrides. Molybdenum nitrides were synthesized by reaction of 1 mmol of $MoCl_4$ and 10 mmol of $NaNH_2$ (Aldrich, 98%) in argon-filled glove box. The total mass of these powder was less than 700 mg. **Caution! An intense exothermic reaction occurs suddenly by mixing these powders. Synthesis using a large amount of the starting materials may cause a serious accident.** First, black $MoCl_4$ powder and magnetic stirrer were put in the autoclave, and white $NaNH_2$ powder was added. The reaction was subsequently initiated by magnetic stirring (please see the attached movie; the experiment for recording this movie was exceptionally performed without closing the autoclave). Under ambient atmosphere, the product was washed with ethanol and distilled water to remove the

NaCl byproducts and unreacted starting materials, and then filtered. Then, the samples were further washed with approximately 10 ml of acetic acid (ca. 20 vol %; diluted aqueous solution from commercial acetic acid (Kanto, 99.7 %)), then washed again with ethanol and water. For the synthesis of manganese molybdenum nitride, 0.3-1.5 mmol of $MnCl_2$ (Sterm, 97%) and $MoCl_4$ was mixed in an argon-filled glove box, and placed into autoclave with 10 mmol of $NaNH_2$. Thereafter, the same procedure as described above was performed. The synthesis of molybdenum nitride with other metals was attempted in the same way employing 0.3 mmol of $CoCl_2$ (Kanto, 95%) or $FeCl_2$ (Sterm, 98%).

To compute the reaction thermodynamics of these self-combustion reactions, we used density functional theory calculations, leveraging Materials Project data for known compounds, and with formation energies of gaseous H_2O, NH_3, and N_2 referenced to the calorimetry results[41], using the method[42]. Supplemental Information 1 shows benchmarked ammonolysis reactions, showing good agreement with calculated reaction energies and calorimetry results. To compute the formation enthalpy of the disordered γ-$Mo_{0.875}Mn_{0.125}N_{0.5}$ phase, we sampled 100 randomly disordered structures on a 2×2×2 primitive rocksalt structure; using a 1:7 ratio of Mn:Mo on the cation sublattice, and a 1:1 ratio of N:Vacancy on the anion sublattice. We assume that these 100 calculations statistically sample the structural density of states of the disordered structure. Because the 2×2×2 primitive lattice represents small unit cells, we compute the total energy of the disordered γ-$Mo_{0.875}Mn_{0.125}N_{0.5}$ as a microcanonical ensemble formed from a sum of smaller canonical ensembles, following the methodology,[43] by the equation:

$$\langle E \rangle = \sum_i \exp(-E_i / k_B \mathrm{T})$$

Where $\langle E \rangle$ is the energy of the microcanonical γ-$Mo_{0.875}Mn_{0.125}N_{0.5}$ phase, i represents a single ordered γ-$Mo_{0.875}Mn_{0.125}N_{0.5}$ configuration in a 2x2x2 primitive cell, and E_i is the energy of that configuration.

Total energies were calculated in DFT using the Vienna *ab initio* software package (VASP),[44-45] using the projector augmented-wave method with the GGA-PBE functional. Plane-wave basis cut-off energies are set to 520 eV. The k-point densities were distributed within the Brillouin zone in a Monkhorst-Pack grid,[46] and used default *k*-point densities in compliance with Materials Project calculation standards, which were calibrated to achieve total energy conver-

gence of better than 0.5 meV/atom. Each structure is initiated in ferromagnetic spin configurations. Phase stability calculations are computed using the phase diagram analysis package in Pymatgen,[47] calculated with respect to known nitride phases from the Materials Project.
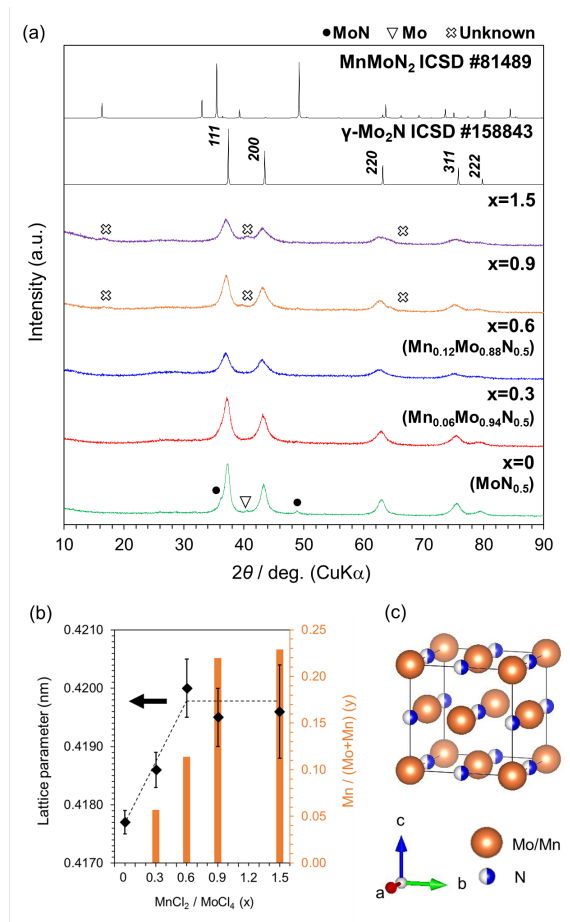
Results and Discussion

Figure 1. (a) The XRD patterns of synthesized manganese molybdenum nitrides with various molar ratio of $MnCl_2/MoCl_4$ in the starting materials represented as x: The $MnCl_2/MoCl_4/NaNH_2$ ratio was 0~1.5: 1: 10. **(b)** The lattice parameters and Mn content of synthesized products from the molar ratio of $MnCl_2/MoCl_4$. The atomic ratios of the product determined by EDX, y, were shown as bars. **(c)** Crystal structure of synthesized $Mn_yMo_{1-y}N_{0.5}$.

The mixing of $MoCl_4$, $MnCl_2$, and $NaNH_2$ initiated an intense exothermic reaction, resulting in the formation of black powder. This black powder was characterized after washing with distilled water and subsequent acetic-acid treatment. $NaNH_2$ converted into NaOH by washing with distilled water, and NaCl, manganese residuals and other magnesium-rich compounds can be removed by water and acid treatments. Typical yield was 20-30 mass % based on molybdenum; it was difficult to take all the product after the filtration. The persistence of the ternary molybdenum nitride

products indicates chemical stability against water and strong bases. Moreover, subsequent acid treatment also demonstrated stability towards weak acids. Figure 1 shows the X-ray diffraction patterns of the products synthesized with various molar ratio of $MoCl_4/MnCl_2$, where the molar ratio of $MnCl_2/MoCl_4$ in the starting materials is defined as x. In all products, the main peaks could be indexed as cubic γ-Mo_2N. No diffraction peaks corresponding to β-Mo_2N, $MnMoN_2$, Mn_2N was observed.

In x=0, cubic γ-Mo_2N and impurities, MoN and Mo metal, were detected. The lattice parameters of cubic γ-Mo_2N increased linearly from $x = 0$ to $x = 0.6$, but did not change within the error bar between $x = 0.6$ and 1.5. The Mn/(Mn+Mo) ratios of the products were semi-quantitatively determined by EDX were lower than $MnCl_2/MoCl_4$ ratio in starting mixtures; the compositions determined by SEM-EDX and STEM-EDX agreed well. This Mn/(Mn+Mo) ratio increased with increasing the ratio of $MnCl_2/MoCl_4$ from o to 0.6. Thus, the change in lattice parameters and elemental analysis suggest random Mn substitution for the Mo site in γ-Mo_2N at $x = 0.3$ and $x = 0.6$. Please note that the ratios of manganese in the product is smaller than those reported in x, suggesting that only partial manganese is in the product and other manganese should be removed after washing with distilled water and acid treatment. Hereafter, these products with x=0, 0.3 and 0.6 are expressed as $Mn_yMo_{1-y}N_{0.5}$ (y=0, 0.06 and 0.12), respectively, according to EDX analysis.

Nonetheless, since all the diffraction peaks were broad, we cannot analyze the detail of crystal structure. The crystalline size estimated from Scherrer equation from the strongest peaks were 5-6 nm. Nonetheless, this does not ensure the crystalline size of the synthesized nitrides since many local configuration with small energy differences, which was suggested by DFT calculation described in later, could bring about broad diffraction peaks. The possibility of manganese nitrides with small particle size less than 5 nm is difficult to deny from these XRD patterns. Nonetheless, this is unlikely because acid wash after the combustion synthesis should remove such nanoparticles and no manganese-rich region were detected in STEM-EDX as below. There are additional broad diffraction peaks which cannot be assigned as a cubic phase were observed for $x \geqq 0.9$. These diffraction peaks for $x \geqq 0.9$ can be attributed to the partial ordering of Mn and

Mo since the angles of unindexed peaks were close to layered $MnMoN_2$, where Mn and Mo layers stack alternatively.
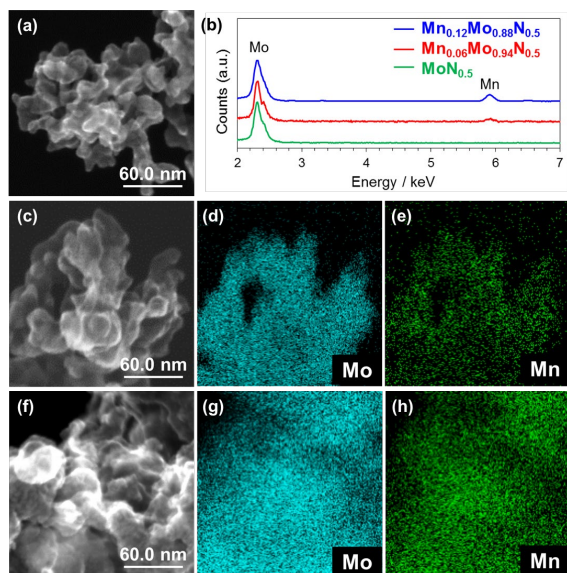

Figure 2 (a) STEM image of $MoN_{0.5}$. **(b)** EDX spectrums of products. **(c)** STEM image, and EDX mapping of **(d)** Mo and **(e)** Mn for $Mn_{0.06}Mo_{0.94}N_{0.5}$ sample. **(f)** STEM image, and EDX mapping of **(g)** Mo and **(h)** Mn for $Mn_{0.12}Mo_{0.88}N_{0.5}$ sample.

The scanning transmission electron microscopy (STEM) images of $Mn_yMo_{1-y}N_{0.5}$ products (y=0, 0.06 and 0.12) are shown in Figure 2 (a, c, f). The size of particles forming aggregates increased with an increase in the molar ratio of $MnCl_2/MoCl_4$. These approximate particle sizes were estimated to be 20 nm for $MoN_{0.5}$, 30-40 nm for $Mn_{0.06}Mo_{0.94}N_{0.5}$, and 50 nm for $Mn_{0.12}Mo_{0.88}N_{0.5}$, respectively. Figure 2 (b) shows the energy dispersive X-ray spectrometry (EDX) spectrum of products. The EDX peaks of Mo (Lα: 2.293 keV) and Mn (Kα: 5.894 keV) were detected for $Mn_{0.06}Mo_{0.94}N_{0.5}$ and $Mn_{0.12}Mo_{0.88}N_{0.5}$ samples. On the other hand, no manganese was detected for $MoN_{0.5}$. STEM-EDX mapping images of manganese molybdenum nitrides are shown in Figure 2 (c-e) for $Mn_{0.06}Mo_{0.94}N_{0.5}$ and (f-h) for $Mn_{0.12}Mo_{0.88}N_{0.5}$. Molybdenum and manganese showed almost similar distribution, which indicate Mn-substituted $MoN_{0.5}$.

γ-Mo_2N is the high-temperature polymorph of Mo_2N, and so the formation of the γ- phase instead of the β- or δ-phases suggests that the temperature of the self-combustion synthesis reaction exceeds 673-1123 K.[49-50] The presence

of manganese could change the order/disorder transition temperature, but this effect is likely small, due to the relatively small fraction of Mn in solid-solution. During combustion, the temperature rises quickly and is then quenched rapidly. Thus, there is compelling possibility that any high-temperature phases formed during combustion synthesis can be retained in a metastable state at ambient conditions. Although $MnMoN_2$ is a stable phase in the predicted Mo-Mn-N phase diagram, high-temperatures promote metal reduction by evolution of gaseous N_2, driving phase equilibrium towards the nitrogen-poor intermetallic subnitrides, such as $MoN_{0.5}$.[51] It is possible that metathesis reactions carried out under high-pressures may facilitate the formation of nitrogen-rich nitrides,[52-53] which could enable interesting semiconducting properties in these ternary mixed-transition metal nitrides.

To determine the thermodynamic (meta)stability of Mn-substituted Mo_2N, we used density functional theory (DFT) to model the formation energies of 100 disordered γ-$Mn_{0.12}Mo_{0.88}N_{0.5}$ structures on a 2×2×2 primitive rocksalt structure as described previously in the **Methods** section. The Mo-Mn-N phase diagram and a $Mo_{0.875}Mn_{0.125}N_{0.5}$ structural density of states is shown in **Figure 3**. The canonical ensemble-averaged formation enthalpy of $Mo_{0.875}Mn_{0.125}N_{0.5}$ is metastable by ΔH_{decomp} = 11.7 kJ/mol at room temperature with respect to $Mn_2N + MoN + Mo$, and metastable by ΔH_{decomp} = 13.6 kJ/mol at 1000K. By the ideal solution model, the maximal configurational entropy of $Mo_{0.875}Mn_{0.125}N_{0.5}$ is $S_{config} = S_{anion} + S_{cation}$ = 13.4 J/mol K. This means that disordered $Mo_{0.875}Mn_{0.125}N_{0.5}$ can be stabilized at temperatures > 1000K through its Gibbs free-energy , but is metastable if quenched to ambient conditions. To the best of our knowledge, γ-$Mn_{0.12}Mo_{0.88}N_{0.5}$ has not been previously reported in the literature.

From the DFT-computed formation enthalpy of $Mo_{0.875}Mn_{0.125}N_{0.5}$, we compute the solid-state metathesis reaction conducted here to be highly exothermic (ΔH = -253 kJ/mol), as shown in Table. 1, enabling it to proceed spontaneously at room temperature. On the other hand, the reaction enthalpy of the corresponding ammonolysis of oxides would be endothermic (ΔH = 49 kJ/mol), but could potentially be initiated at high-temperature by the production of H_2O and N_2 gases, providing entropy on the product side of the reaction to drive the formation of $Mo_{0.875}Mn_{0.125}N_{0.5}$. Nevertheless, between these two synthesis methods, combustion synthesis appears to be the simpler and more facile route to these novel ternary nitride compounds.
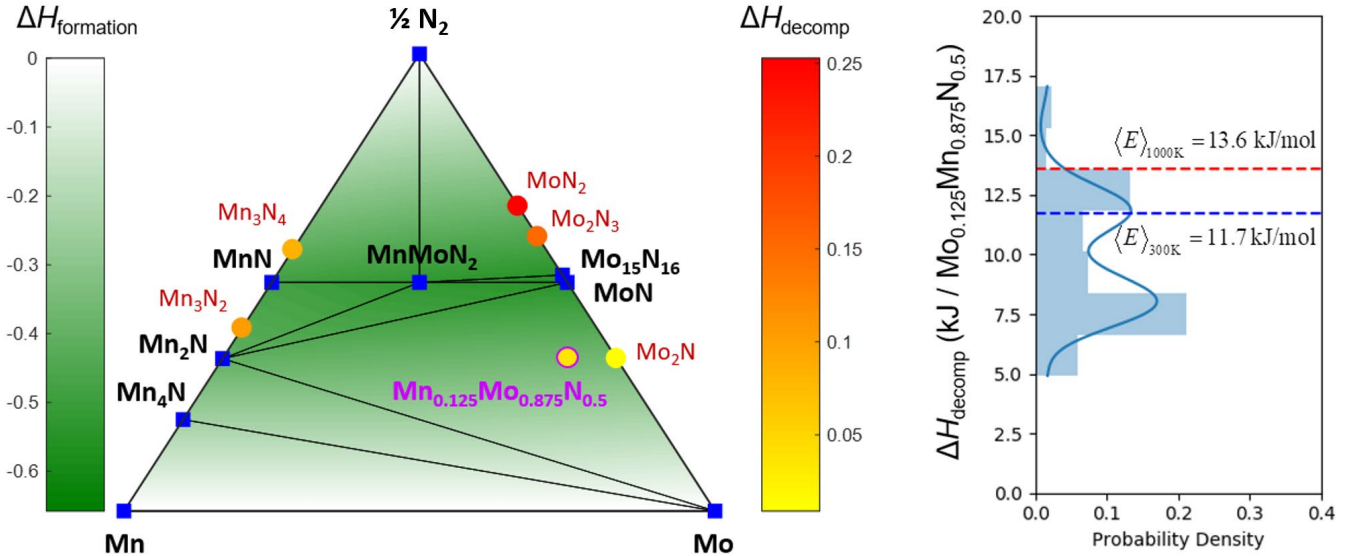
Figure 3 a.) Ternary phase diagram of Mo-Mn-N space, where $Mn_{0.125}Mo_{0.875}N_{0.5}$ is highlighted in purple. Blue squares indicate stable phases, yellow-red circles are metastable phases with decomposition enthalpies noted in eV/atom, green shading indicates formation energy of the convex hull in eV/atom. b.) Structural density of states of disordered γ-$Mn_{0.125}Mo_{0.875}N_{0.5}$. Blue and red lines indicate canonical ensemble-averaged enthalpies of the disordered phases at 300 and 1000K, respectively.

Table 1. DFT-computed reaction enthalpies of oxide ammonolysis versus self-combustion metathesis reactions for $Mo_{1-y}Mn_yN_{0.5}$.

Reaction Type	Balanced Reaction	ΔH_{rxn} (kJ/$Mo_{1-y}Mn_yN_{0.5}$)
Ammonolysis of metal oxides	$MoO_3 + 2NH_3(g)+ \rightarrow MoN_{0.5} + 3 H_2O(g) + 3/4 N_2(g)$	50
	$1/8 MnO_2 + 7/8 MoO_3 + 23/12 NH_3(g) \rightarrow Mn_{0.125}Mo_{0.875}N_{0.5} + 23/8 H_2O(g) + 17/24 N_2(g)$	49
Combustion metathesis	$MoCl_4 + 4 NaNH_2 \rightarrow MoN_{0.5} + 4 NaCl + 8/3 NH_3(g) + 5/12 N_2(g)$	-285
	$1/8 MnCl_2 + 7/8 MoCl_4 + 15/4 NaNH_2 \rightarrow Mn_{0.125}Mo_{0.875}N_{0.5} + 15/4 NaCl + 5/2 NH_3(g) + 3/8 N_2(g)$	-253

In order to examine the effect of Mn-substitution on the electronic structure of $MoN_{0.5}$, magnetic properties of the products were investigated by a vibrating sample magnetometer (VSM). Figure 4 shows the temperature dependence of the magnetic moment of synthesized manganese molybdenum nitride $Mn_yMo_{1-y}N_{0.5}$ (y=0, 0.06 and 0.12). The sample with $MoN_{0.5}$ showed diamagnetic signal at approximately 5 K, suggesting the appearance of superconductivity.[54] This is further evidence of γ-Mo_2N with a random occupation of nitrogen.[40] On the other hand, $Mn_{0.06}Mo_{0.94}N_{0.5}$ and $Mn_{0.12}Mo_{0.88}N_{0.5}$ did not show diamagnetic signal, indicating the disappearance of superconductivity. This change in magnetic moment indicates a modification of the electronic structure in Mn-substituted $MoN_{0.5}$.

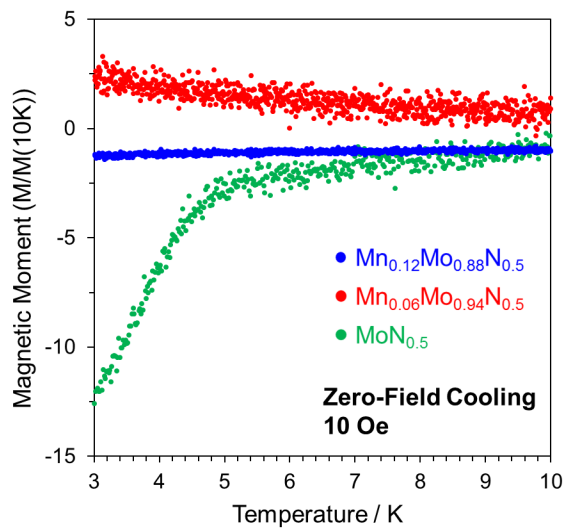**Figure 4** Temperature dependence of magnetic moment for MoN$_{0.5}$ (green), Mn$_{0.06}$Mo$_{0.94}$N$_{0.5}$ (red) and Mn$_{0.12}$Mo$_{0.88}$N$_{0.5}$ (blue).

Our synthesis of ternary molybdenum nitrides was further generalized from MnCl$_2$ to CoCl$_2$ and FeCl$_2$ (Figure S2). The lattice parameters of γ-Mo$_2$N phase were 0.4166(1) nm and 0.4185(1) nm for Co-Mo and Fe-Mo nitrides, respectively, which were different from that of MoN$_{0.5}$ (a=0.4177(2) nm). Co and Fe were homogeneously distributed, suggesting the incorporation of Co and Fe into γ-Mo$_2$N (Figure S3). Although these syntheses always accompany with the formation of metals and δ–MoN and thus the synthesis of single-phase γ-Mo$_2$N phase remains a further challenge, this synthesis method can be expanded as a general approach for producing ternary molybdenum nitrides.
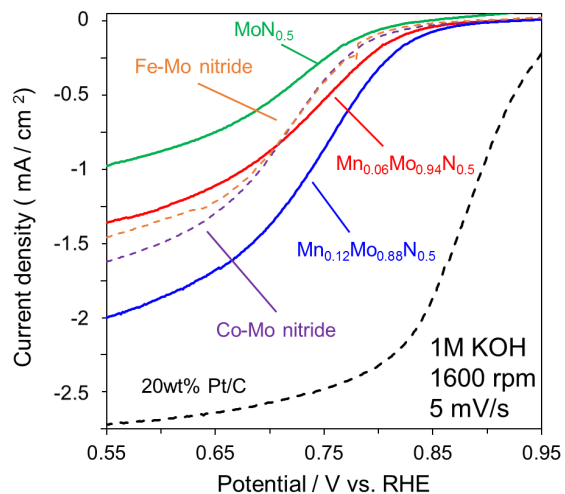
Figure 5 Linear-sweep polarization curves of products for $MoN_{0.5}$ (green), $Mn_{0.06}Mo_{0.94}N_{0.5}$ (red), $Mn_{0.12}Mo_{0.88}N_{0.5}$ (blue), Fe-Mo nitride (orange), and Co-Mo nitride (purple) recorded with a rotating disc electrode in O_2-saturated 1M KOH solution at a sweep rate of 5 mV s^{-1}. The polarization curve of 20 wt.% Pt/C is shown for comparison.

Finally, we explored the potential electrocatalytic applications of our ternary molybdenum nitrides for the oxygen reduction reaction (ORR). The ternary molybdenum nitrides synthesized in this study have <50 nm particle size and appear kinetically resistant against corrosion in alkaline solutions. Figure 5 shows the oxygen reduction reaction activity of $MoN_{0.5}$ and its Mn-, Co-, and Fe- substituted ternaries in a 1 M KOH aqueous solution, and also includes for reader's reference a dashed line for 20 wt% Pt/C. γ-$MoN_{0.5}$ exhibited the lowest catalytic activity, and its activity was enhanced by introducing the 3d transition metals. Catalytic activity improved with increasing Mn content, and $Mn_{0.12}Mo_{0.88}N_{0.5}$ showed the lowest overpotential and the highest current density, even though it had the largest nanoparticle size ($Mo_2N \sim 20$ nm, $Mn_{0.12}Mo_{0.88}N_{0.5} \sim 50$ nm; Figure 2 a,c,f). Although these catalytic activities are not high as commercial Pt/C, we demonstrate here that substitution of 3*d* transition metals improves the catalytic performance of γ-Mo_2N, which is likely due to modification of the electronic structure via these transition metal substitutions on the Mo site. By extending the known binary metal nitrides into ternary compositions, we can access a broader structure-property design space for enhanced materials functionality.

Conclusion

Low-temperature synthesis methods are in great demand for scalable and sustainable materials synthesis. In this paper, we demonstrated a facile self-combustion synthesis method for the realization of new ternary molybdenum nitrides. These reactions initiate at room temperature, but rapidly reach high temperatures and are then quenched shortly thereafter. The non-equilibrium nature of this process enables the formation of metastable disordered nitrides with emergent properties. Notably, introduction of manganese into molybdenum nitrides was found to enhance ORR activity compared to pristine γ-Mo_2N. Incorporation of iron and cobalt into γ-Mo_2N was also demonstrated, suggesting that this self-combustion synthesis method can be expanded as a general approach for the rapid exploration of novel ternary metal nitride materials. Our DFT investigation yielded thermochemical insights into this highly exothermic reaction, and can be generally applied to screen for and identify similar self-combustion metathesis reactions. Finally, the combined experimental and computational investigation here offers a general paradigm for the predictive synthesis of novel functional materials.

ASSOCIATED CONTENT

Supporting Information

Detailed characterization methods are described in Supporting Information.

AUTHOR INFORMATION

Corresponding Authors

Wenhao Sun: wenhaosun@lbl.gov

Akira Miura: amiura@eng.hokudai.ac.jp

ACKNOWLEDGMENT

REFERENCES

1.   Wenhao Sun; Christopher Bartel; Elisabetta Arca; Sage Bauers; Bethany Matthews; Bernardo Orvañanos; Bor-Rong Chen; Michael F. Toney; Laura T. Schelhas; William Tumas; Janet Tate; Andriy Zakutayev; Stephan Lany; Aaron Holder; Ceder, G., A Map of the Inorganic Ternary Metal Nitrides. *arXiv preprint* **2018**, arXiv:1809.09202.

2.   Tareen, A. K.; Priyanga, G. S.; Behara, S.; Thomas, T.; Yang, M., Mixed ternary transition metal nitrides: a comprehensive review of synthesis, electronic structure, and properties of engineering relevance. *Prog. Solid State Chem.* **2019,** *53*, 1-26.

3.   Höhn, P.; Niewa, R., Nitrides of Non-Main Group Elements. In *Handbook of Solid State Chemistry*, Dronskowski, R.; Kikkawa, S.; Stein, A., Eds. 2017.

4.   DiSalvo, F. J.; Clarke, S. J., Ternary nitrides: a rapidly growing class of new materials. *Curr. Opin. Solid State Mater. Sci.* **1996,** *1* (2), 241-249.

5.   Veprek, S.; Reiprich, S., A concept for the design of novel superhard coatings. *Thin Solid Films* **1995,** *268* (1), 64-71.

6.   Paseuth, A.; Yamagata, K.; Miura, A.; Higuchi, M.; Tadanaga, K.; Cinibulk, M., Deposition and Analysis of Al-Rich c-$Al_xTi_{1-x}N$ Coating with Preferred Orientation. *J. Am. Ceram. Soc.* **2017,** *100* (1), 343-353.

7.   Gudat, A.; Kniep, R.; Rabenau, A.; Bronger, W.; Ruschewitz, U., Li3FeN2, a ternary nitride with $1\infty[FeN423-]$ chains: Crystal structure and magnetic properties. *Journal of the Less Common Metals* **1990,** *161* (1), 31-36.

8.   Houben, A.; Burghaus, J.; Dronskowski, R., The Ternary Nitrides GaFe3N and AlFe3N: Improved Synthesis and Magnetic Properties. *Chem. Mater.* **2009,** *21* (18), 4332-4338.

9.   Bhattacharyya, S., Iron Nitride Family at Reduced Dimensions: A Review of Their Synthesis Protocols and Structural and Magnetic Properties. *The Journal of Physical Chemistry C* **2015,** *119* (4), 1601-1622.

10.   Vaughn Ii, D. D.; Araujo, J.; Meduri, P.; Callejas, J. F.; Hickner, M. A.; Schaak, R. E., Solution Synthesis of Cu3PdN Nanocrystals as Ternary Metal Nitride Electrocatalysts for the Oxygen Reduction Reaction. *Chem. Mater.* **2014,** *26* (21), 6226-6232.

11.   Hada, K.; Nagai, M.; Omi, S., Characterization and HDS Activity of Cobalt Molybdenum Nitrides. *The Journal of Physical Chemistry B* **2001,** *105* (19), 4084-4093.

12.   Sage R. Bauers; Aaron Holder; Wenhao Sun; Celeste L. Melamed; Rachel Woods-Robinson; John Mangum; John Perkins; William Tumas; Brian Gorman; Adele Tamboli; Gerbrand Ceder; Stephan Lany; Zakutayev, A., Ternary Nitride Semiconductors in the Rocksalt Crystal Structure. *arXiv preprint* **2018**, arXiv:1810.05668.

13.   Arca, E.; Lany, S.; Perkins, J. D.; Bartel, C.; Mangum, J.; Sun, W.; Holder, A.; Ceder, G.; Gorman, B.; Teeter, G.; Tumas, W.; Zakutayev, A., Redox-Mediated Stabilization in Zinc Molybdenum Nitrides. *J. Am. Chem. Soc.* **2018,** *140* (12), 4293-4301.

14.   Bem, D. S.; LampeOnnerud, C. M.; Olsen, H. P.; zurLoye, H. C., Synthesis and structure of two new ternary nitrides: FeWN2 and MnMoN2. *Inorg. Chem.* **1996,** *35* (3), 581-585.

15.   Miura, A.; Wen, X.-D.; Abe, H.; Yau, G.; DiSalvo, F. J., Non-stoichiometric Fe_xWN_2: Leaching of Fe from layer-structured $FeWN_2$. *J. Solid State Chem.* **2010,** *183* (2), 327-331.

16.   Alconchel, S.; Sapina, F.; Beltran, D.; Beltran, A., Chemistry of interstitial molybdenum ternary nitrides MnMo3N (M = Fe, Co, n = 3; M = Ni, n = 2). *J. Mater. Chem.* **1998,** *8* (8), 1901-1909.

17.   Miura, A.; Tadanaga, K.; Magome, E.; Moriyoshi, C.; Kuroiwa, Y.; Takahiro, T.; Kumada, N., Octahedral and trigonal-prismatic coordination preferences in Nb-, Mo-, Ta-, and W-based ABX_2 layered oxides, oxynitrides, and nitrides. *J. Solid State Chem.* **2015,** *229*, 272-277.

18.   Rauch, P. E.; DiSalvo, F. J.; Brese, N. E.; Partin, D. E.; O'Keeffe, M., Synthesis and Neutron Diffraction Study of Na3WN3 and Na3MoN3. *J. Solid State Chem.* **1994,** *110* (1), 162-166.

19.   Yamane, H.; DiSalvo, F. J., Synthesis and crystal structure of Sr2ZnN2 and Ba2ZnN2. *J. Solid State Chem.* **1995,** *119* (2), 375-379.

20.   Miura, A.; Takei, T.; Kumada, N.; Wada, S.; Magome, E.; Moriyoshi, C.; Kuroiwa, Y., Bonding Preference of Carbon, Nitrogen, and Oxygen in Niobium-Based Rock-Salt Structures. *Inorg. Chem.* **2013,** *52*, 9699-9701.

21.   Wang, H.; Li, W.; Zhang, M., New Approach to the Synthesis of Bulk and Supported Bimetallic Molybdenum Nitrides. *Chem. Mater.* **2005,** *17* (12), 3262-3267.

22.   Jacobsen, C. J. H.; Zhu, J. J.; Lindeløv, H.; Jiang, J. Z., Synthesis of ternary nitrides by mechanochemical alloying. *J. Mater. Chem.* **2002,** *12* (10), 3113-3116.

23.   Wang, L.; Xian, W.; Zhang, K.; Liu, W.; Qin, H.; Zhou, Q.; Qian, Y., One-step solid state reaction for the synthesis of ternary nitrides Co3Mo3N and Fe3Mo3N. *Inorg. Chem. Front.* **2017,** *4* (12), 2055-2058.

24.	Treece, R. E.; Macala, G. S.; Kaner, R. B., Rapid synthesis of gallium phosphide and gallium arsenide from solid-state precursors. *Chem. Mater.* **1992,** *4* (1), 9-11.

25.	Gillan, E. G.; Kaner, R. B., Synthesis of Refractory Ceramics via Rapid Metathesis Reactions between Solid-State Precursors. *Chem. Mater.* **1996,** *8* (2), 333-343.

26.	Martinolich, A. J.; Neilson, J. R., Toward Reaction-by-Design: Achieving Kinetic Control of Solid State Chemistry with Metathesis. *Chem. Mater.* **2017,** *29* (2), 479-489.

27.	Parkin, I., *Solid State Metathesis Reaction for Metal Borides, Silicides, Pnictides and Chalcogenides: Ionic or Elemental Pathways.* 1996; Vol. 25.

28.	Miura, A.; Takei, T.; Kumada, N., Synthesis of Wurtzite-Type InN Crystals by Low-Temperature Nitridation of $LiInO_2$ Using $NaNH_2$ Flux. *Crystal Growth & Design* **2012,** *12* (9), 4545-4547.

29.	Miura, A.; Takei, T.; Kumada, N., Low-Temperature Nitridation of Manganese and Iron Oxides Using $NaNH_2$ Molten Salt. *Inorg. Chem.* **2013,** *52* (20), 11787-11791.

30.	Miura, A., Low-temperature synthesis and rational design of nitrides and oxynitrides for novel functional material development. *J. Ceram. Soc. Jpn.* **2017,** *125* (7), 552-558.

31.	Miura, A.; Lowe, M.; Leonard, B. M.; Subban, C. V.; Masubuchi, Y.; Kikkawa, S.; Dronskowski, R.; Hennig, R. G.; Abruña, H. D.; DiSalvo, F. J., Silver delafossite nitride, $AgTaN_2$? *J. Solid State Chem.* **2011,** *184* (1), 7-11.

32.	Todd, P. K.; Neilson, J. R., Selective formation of yttrium manganese oxides through kinetically competent assisted metathesis reactions. *J. Am. Chem. Soc.* **2019**.

33.	McKay, D.; Hargreaves, J. S. J.; Rico, J. L.; Rivera, J. L.; Sun, X. L., The influence of phase and morphology of molybdenum nitrides on ammonia synthesis activity and reduction characteristics. *J. Solid State Chem.* **2008,** *181* (2), 325-333.

34.	WILEY, J. B.; KANER, R. B., Rapid Solid-State Precursor Synthesis of Materials. *Science* **1992,** *255* (5048), 1093-1097.

35.	Odahara, J.; Miura, A.; Rosero-Navarro, N. C.; Tadanaga, K., Explosive Reaction for Barium Niobium Perovskite Oxynitride. *Inorg. Chem.* **2018,** *57* (1), 24-27.

36.	Song, B.; Chen, X.; Han, J.; Jian, J.; Wang, W.; Zuo, H.; Zhang, X.; Meng, S., Facile Route to Nitrides: Transformation from Single Element to Binary and Ternary Nitrides at Moderate Temperature through a New Modified Solid-State Metathesis. *Inorg. Chem.* **2009,** *48* (22), 10519-10527.

37.	Miura, A.; Tague, M. E.; Gregoire, J. M.; Wen, X.-D.; van Dover, R. B.; Abruña, H. c. D.; DiSalvo, F. J., Synthesis of Pt−Mo−N Thin Film and Catalytic Activity for Fuel Cells. *Chem. Mater.* **2010,** *22* (11), 3451-3456.

38.	Cao, B.; Neuefeind, J. C.; Adzic, R. R.; Khalifah, P. G., Molybdenum nitrides as oxygen reduction reaction catalysts: structural and electrochemical studies. *Inorg. Chem.* **2015,** *54* (5), 2128-36.

39.	Cao, B.; Veith, G. M.; Neuefeind, J. C.; Adzic, R. R.; Khalifah, P. G., Mixed close-packed cobalt molybdenum nitrides as non-noble metal electrocatalysts for the hydrogen evolution reaction. *J. Am. Chem. Soc.* **2013,** *135* (51), 19186-92.

40.	Sun, W.; Dacek, S. T.; Ong, S. P.; Hautier, G.; Jain, A.; Richards, W. D.; Gamst, A. C.; Persson, K. A.; Ceder, G., The thermodynamic scale of inorganic crystalline metastability. *Science advances* **2016,** *2* (11), e1600225-e1600225.

41.	Elder, S. H.; DiSalvo, F. J.; Topor, L.; Navrotsky, A., Thermodynamics of ternary nitride formation by ammonolysis: application to lithium molybdenum nitride (LiMoN2), sodium tungsten nitride (Na3WN3), and sodium tungsten oxide nitride (Na3WO3N). *Chem. Mater.* **1993,** *5* (10), 1545-1553.

42.	Wang, L.; Maxisch, T.; Ceder, G., Oxidation energies of transition metal oxides within the $\mathrm{GGA}+\mathrm{U}$ framework. *Physical Review B* **2006,** *73* (19), 195107.

43.	Yang, K.; Oses, C.; Curtarolo, S., Modeling Off-Stoichiometry Materials with a High-Throughput Ab-Initio Approach. *Chem. Mater.* **2016,** *28* (18), 6484-6492.

44.	Kresse, G.; Furthmüller, J., Efficient iterative schemes for ab initio total-energy calculations using a plane-wave basis set. *Physical Review B* **1996,** *54* (16), 11169-11186.

45.	Kresse, G.; Furthmüller, J., Efficiency of ab-initio total energy calculations for metals and semiconductors using a plane-wave basis set. *Computational Materials Science* **1996,** *6* (1), 15-50.

46.	Monkhorst, H. J.; Pack, J. D., Special points for Brillouin-zone integrations. *Physical Review B* **1976,** *13* (12), 5188-5192.

47.	Ong, S. P.; Richards, W. D.; Jain, A.; Hautier, G.; Kocher, M.; Cholia, S.; Gunter, D.; Chevrier, V. L.; Persson, K. A.; Ceder, G., Python Materials Genomics (pymatgen): A robust, open-source python library for materials analysis. *Computational Materials Science* **2013,** *68*, 314-319.

48.   Inumaru, K.; Baba, K.; Yamanaka, S., Synthesis and Characterization of Superconducting β-Mo2N Crystalline Phase on a Si Substrate: An Application of Pulsed Laser Deposition to Nitride Chemistry. *Chem. Mater.* **2005,** *17* (24), 5935-5940.

49.   Ettmayer, P., Das System Molybdän-Stickstoff. *Monatshefte für Chemie / Chemical Monthly* **1970,** *101* (1), 127-140.

50.   Jehn, H.; Ettmayer, P., The molybdenum-nitrogen phase diagram. *Journal of the Less Common Metals* **1978,** *58* (1), 85-98.

51.   Sun, W.; Holder, A.; Orvañanos, B.; Arca, E.; Zakutayev, A.; Lany, S.; Ceder, G., Thermodynamic Routes to Novel Metastable Nitrogen-Rich Nitrides. *Chem. Mater.* **2017,** *29* (16), 6936-6946.

52.   Lei, L.; Yin, W.; Jiang, X.; Lin, S.; He, D., Synthetic Route to Metal Nitrides: High-Pressure Solid-State Metathesis Reaction. *Inorg. Chem.* **2013,** *52* (23), 13356-13362.

53.   Horvath-Bordon, E.; Riedel, R.; Zerr, A.; McMillan, P. F.; Auffermann, G.; Prots, Y.; Bronger, W.; Kniep, R.; Kroll, P., High-pressure chemistry of nitride-based materials. *Chem. Soc. Rev.* **2006,** *35* (10), 987-1014.

54.   Matthias, B. T.; Hulm, J. K., A Search for New Superconducting Compounds. *Phys. Rev.* **1952,** *87* (5), 799-806.
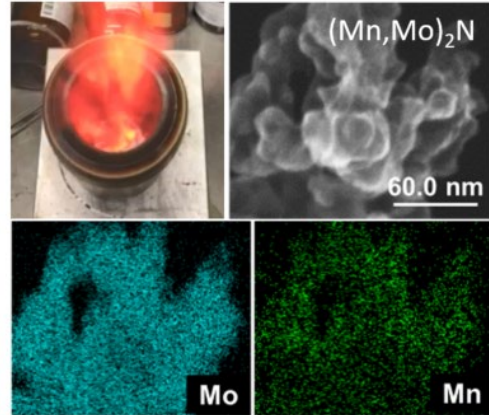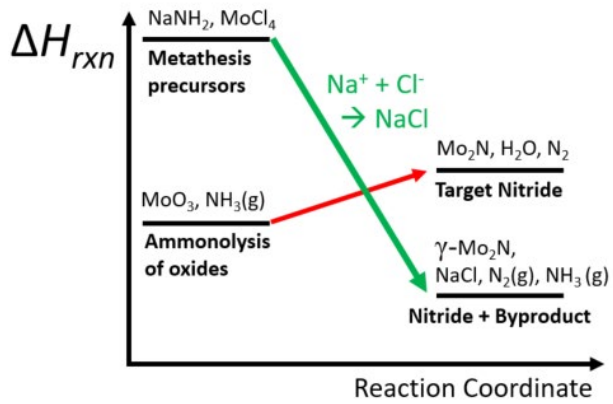
Self-combustion synthesis is a simple but powerful approach for emerging novel metastable ternary molybdenum nitrides.